INTERNATIONAL SCIENTIFIC JOURNAL OF ENGINEERING AND MANAGEMENT ISSN: 2583-6129
VOLUME: 03 ISSUE: 06 | JUNE – 2024 DOI: 10.55041/ISJEM02089
AN INTERNATIONAL SCHOLARLY || MULTIDISCIPLINARY || OPEN ACCESS || INDEXING IN ALL MAJOR DATABASE & METADATA

PV Based Modified SEPIC Converter Fed BLDC Motor

1st M. Madeshwaran, 2nd Dr. T. R. Sumithira

[1] PG Scholar, Department of EEE, Government College of Engineering Salem, Tamil Nadu, India.
[2] Assistant Professor, Department of EEE, Government College of Engineering Salem, Tamil Nadu, India.

[1] Government College of Engineering, Salem, Tamil Nadu, India.
[1]Madeshwaranbe1999@gmail.com,

Abstract - A PV based modified SEPIC converter for microgrid applications is developed to increase the reliability and to reduce the operating cost of Electric vehicle. In the modern area, people are facing problems like pollution and outage of fossil fuels which may become reason for the human destruction. PV modified based SEPIC Converter fed Electric vehicle can run without use of any Charging stations. Here the number of PV Arrays used can also be reduced by using SEPIC Converter, and the voltage can be boosted. SEPIC converter is placed in between PV array and Battery of Electric vehicle. Use of (VSI) Voltage Source Inverter helps and it to vary the speed of Electric vehicle smoothly in steps. The proposed converter is able to attain a higher voltage gain in comparison with similar previous transformer-less DC–DC converters. Also, the proposed converter presents low-voltage stress across the switch and output diode. The proposed converter is controlled through a single switch and there is no limitation for a range of duty ratios. The voltage gain analysis of the proposed converter is done in continuous conduction mode and discontinuous conduction mode, also comparative analysis is done with the existing topologies with similar features. BLDC motors are known for their high performance, and long lifespan. minimize the cost of PV system-wide power generation while also improving the system's performance. All the simulation work is done in MATLAB.

Index Terms - Modified SEPIC Converter (MSC), DC-DC Converter, PV system, BLDC Motor.

I. INTRODUCTION

In the last decade, because of environmental difficulties and deficiency of traditional fossil fuels such as oil and coal, renewable energy sources (RESs) often called alternative energy such as fuel cells, wind energy, photovoltaic (PV), and energy storage systems (ESSs) have been more preferable [1]. Nevertheless, due to the intermittent feature of RES, they are not able to generate the desired level of the output voltage. For instance, the PV modules generate a variable and low voltage (about 20–45 V), which is not enough for high-voltage applications such as DC microgrids, DC home appliances, and grid-connected AC utilities [2]. Also, the high voltage needed in electric vehicles cannot be supplied by supercapacitors, fuel cells, and batteries directly [3]. Thereupon, power electronics high-voltage step-up DC–DC converters have an essential duty in new energy resources systems [3, 4]. Fig. 1 shows the vital role of DC–DC converters with parallel or series connections to convert low voltage (12–36 V) generated by RES to high voltage (400–800 V) for DC microgrid applications.

Fig.1 Block diagram of MSC Converter.

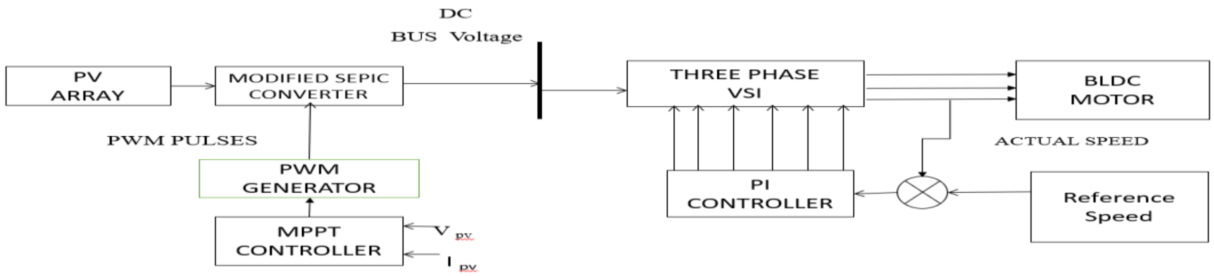

In the recent years, the global warming has increased the awareness on the reduction of carbon dioxide (CO_2) emission from the transportation vehicles, which has a strong impact on the global warming. The emissions of CO_2 are mainly due to the usage of internal combustion (IC) engines in the transportation vehicle. SEPIC is a DC to DC converter and is capable of operating in either step up or step down mode and widely used in battery operated equipment by varying duty cycle of gate signal of MOSFET. Nonconventional energy sources are biomass, tidal, and geothermal energy sources that exist in nature in particular regional sectors. But solar and wind energies are abundant in nature and available in all regional sectors. Especially, solar and wind energy sources give maximum efficiency and reliability when compared with other nonconventional energy sources. Moreover, the upcoming research focuses on these two renewable energy sectors integrated to the AC and DC grids Traditional pulse-width modulation DC–DC boost, CUK, ZETA, buck–boost, and single-ended primary-inductor capacitor (SEPIC) converters have been widely used for high-power applications [5]. Each structure has its pros and cons, and must be chosen according to its requirements and applications. However, in very-high-voltage applications, conventional step-up converters must operate with their maximum duty cycle value, which causes efficiency reduction and operation malfunction [6]. As a result, the highest boost factor in these converters cannot exceed 4–5 in practice [7]. In recent years, improved step-up DC–DC converters with higher boost ability have been proposed. A high-frequency transformer has been utilised in isolated DC–DC converters to attain high-voltage gain by controlling its turn's ratio [8–10].Nonetheless, high-voltage stress across the secondary side, ripple input current, large size, and leakage current of the transformer are the main disadvantages of isolated DC–DC converters [11–15]. Using multi-stages [12], multi-cells [13], switched inductors cells, and switched capacitors cells [14–18] in the conventional structures are the most popular techniques for voltage gain lifting in non-isolated DC–DC converters. However, in all these voltage boosting techniques, additional components must be added to attain the desired voltage, which increases circuit complexity, volume, and cost of the converters In [19], a high-gain quadratic buck–boost converter has been proposed by a combination of buck, boost, and buck–boost structures with single switch control. Also, anew quadratic boost converter based on stackable switching stages has been presented in [15] to obtain high-voltage gain with a small duty ratio. It utilises a simple single switch configuration and provides low-voltage stress across capacitors. Although additional components are required in a modular extension of this structure to attain arbitrary gain, which increases the cost and size of the converter.

PROPOSED SYSTEM:

The proposed system presented in this paper is a modeling of PV based modified sepic converter for microgrid applications The modified Sepic converter is a DC-DC converter topology that combines the advantages of the Sepic converter and the Buck-Boost converter. The modified Sepic converter topology consists of a boost stage integrated with conventional converter and a switch (MOSFET) that controls the output voltage. The converter operates in continuous conduction mode (CCM) and and discontinuous conduction mode.

The modelling of the comprises of a single-ended primary-inductor capacitor (SEPIC) converter along with a boosting module to obtain a high-voltage gain. It has all advantages of the SEPIC converter such as continuous input current, which makes it applicable for renewable energy sources such as photovoltaic systems. The proposed converter is able to attain a higher voltage gain in comparison with similar previous transformer-less DC–DC converters. The proposed converter presents low-voltage stress across the switch and output diode. The proposed converter is controlled through a single power electronic switch and there is no limitation for a range of duty ratios. The voltage in controlled through a PI controller module. VSI converter are used to couple the dc link voltage to BLDC motor.

The selection of a suitable maximum power point tracking (MPPT), keeping because of its design complexity for a particular PV system is considered one of the imperative factors. Otherwise, the maximum solar energy will not be harvested by the PV system. Additionally, no. of required sensors, tracking speed, accuracy, efficiency, cost, dynamic response etc. factors are also considered for the selection of suitable MPPT techniques for a particular application and converter configuration. The conventional MPPT technique (perturbation and observation, hill climbing, and incremental conductance) is not able to track the global MPP under continuous changing solar irradiance and partial shading conditions, which reduces overall system efficiency and increases power losses. There are numerous MPPT techniques that have been discussed in the literature, which can be applied to uniform and non-uniform solar irradiation conditions.

Objective:

- To improve the voltage gain of DC-DC converter using appropriate modeling of single-ended primary-inductor capacitor (SEPIC) topology.
- To utilize PV and extract maximum power through PI, MPPT & PI based MPPT.
- To improve performance efficiency of BLDC motor fed EV.

II. LITERATURE SURVEY

Selvi Arumugam et.al., enhance the power transformation stage’s power transfer capabilities and efficiency, improved three-port two step-up single-ended primary-inductor converters (SEPIC) converter fed (Photovoltaic) PV- Hybrid Electric Vehicle was proposed. the proposed converter accepts a wider range of input voltages. The proposed three-port converter uses a multiple-winding high-frequency transformer (HFT) to integrate the dual sources and provide greater voltage gain with lesser elements. Furthermore, by predicting the drive torque need, the power management algorithm (PMA) included with the proposed PV-hybrid electric vehicle (HEV) minimizes the drive motor’s power consumption. An experimental model with a power output of 6kW and a voltage range of 12 to 600 volts has been created and tested. the designed model has 94.11% efficiency. the proposed converter is effective in enhancing a higher range of input voltages. the main advantage of proposed converter circuit is that it has a greater gain for a given duty cycle. In future scope, this topology can also be applied in the various applications which require reduced losses, high power density, and low weight and volume.

Selvarani Natchimuthu et.al., has presents a high gain modified three-port dual boost single-ended primary-inductor converter (SEPIC) converter operated hybrid photovoltaic (PV)/battery electric vehicle to improve the power transfer capability and efficiency of the power conversion stage. The proposed three-port dual boost high gain SEPIC converter accepts wide voltage range of input then the conventional single stage SEPIC converter. the performance of the proposed modified SEPIC converter in boosting the wide range of input voltage. A 6 kW, 12 to 600 V of experimental model has been developed and tested. The SEPIC converter with high frequency transformer offers the isolation between the driving unit and PV power generation system. In addition to this, it provides dual stages of boosting for the output voltage of PV and helps to increase the boosting gain of the conventional SEPIC converter. The power circuit with high frequency transformer and voltage doubler rectifier offers the static gain, which is twice the gain of conventional SEPIC converter. The efficiency of the proposed SEPIC converter is observed as 94.11%.

P. Bhavana et.al., has presented the non-availability of fossil fuels and the shortcomings of nonconventional energy sources taking place in the environment lead the research and development towards alternative and clean energy sources such as renewable energy sources. Renewable or nonconventional energy resources are being used to meet ever-increasing energy demand. The photo voltaic (PV) energy is the right choice of renewable energy for small voltage DC distribution systems, due to their advantages. But this energy source can produce low output power at the utility grid. Hence, to step up this low input voltage to high value for a range of high-voltage applications, DC-DC converters are integrated to the DC microgrids by means of PV system.The present work elaborates the modified SEPIC converter (MSC) designed based on the traditional SEPIC with a boost-up module. In comparison with conventional or traditional SEPIC converter, the proposed MSC produces high voltage gain and continuous current to the DC microgrids. Furthermore, MSC is operated with only one controlled switch. The proposed converter design improves the efficiency, output voltage, and continuous output current of the DC microgrids. The advantages of using MSC topology are addressed. PV system with an MSC configuration continuously generates output current without producing any ripples. This configuration gives the output voltage with high gain, delivers the required amount of power supply demanded by the DC loads, and achieves a reliable power supply to the DC loads by using the integration of an MSC-based PV system. this topology which is well suited for domestic applications. Nowadays, most of the houses are equipped with DC LED lamps, BLDC motor-based ceiling fans, etc.

Aravindha Shilpa.K & Swaroopa.K: has developed a PV based SEPIC Converter fed Electric vehicle (EV) model is created to increase the reliability and to reduce the operating cost of Electric vehicle. Electrification will help reduce vehicular emissions and the usage of any non- renewable Resources. PV based SEPIC Converter fed Electric vehicle can run without use of any Charging stations and also with a very less amount of cost because the combination of PV array with SEPIC Converter reduces the cost. Here the Number of PV Arrays used can also be reduced by using SEPIC Converter, the voltage can be boosted. SEPIC converter is placed in between PV array and Battery of Electric vehicle. Use of (VSI) Voltage Source Inverter helps to vary the speed of Electric vehicle smoothly in steps. which includes a SEPIC converter, is designed to increase power flow from solar PV systems. When and if power is not needed to load, the grid is connected via a DC bus to supply the power generated by PV.

Ioana-Monica Pop-Calimanu & Sorin Popescu and Dan Lascu: has presented a new hybrid SEPIC dc-dc converter with coupled inductors suitable for photovoltaic applications is presented. a static conversion ratio calculation based on which the semiconductor voltage and current stresses are evaluated, leading to the continuous conduction mode (CCM) operation conditions. Finally, an application of the new hybrid converter will consist of a complete solar energy conversion system using a photovoltaic panel. The maximum power point tracking (MPPT) algorithm will be elaborated. As a result, the new topology is suitable in applications where an output voltage much higher than the input voltage is needed.

III. PROPOSED CONVERTER TOPOLOGY

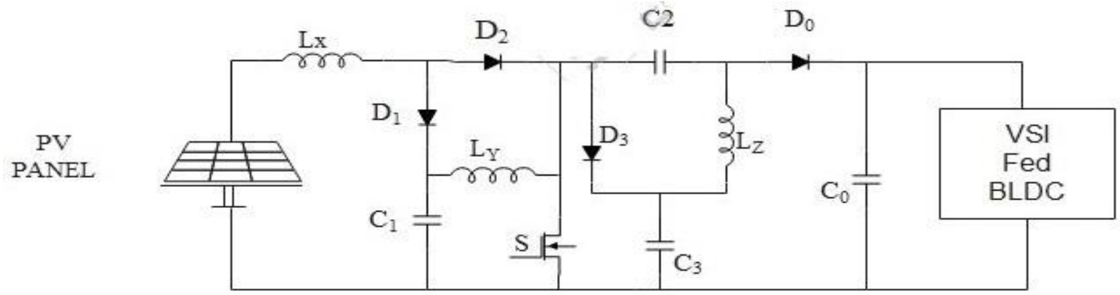

Fig:3: Circuit Diagram for Proposed Modified Sepic Converter.

The circuit configuration of the introduced non-isolated modified SEPIC DC–DC converter. Like a traditional SEPIC converter, the proposed structure includes one input inductor (L_X), one shared ground switch (S), one middle capacitor (C_2), one middle inductor (L_Y), one output diode (D_0), and one output capacitor (C_0). In addition, a voltage-boosting module is embedded between an input inductor and a switch. The boosting module consists of one inductor (L_Y), one capacitor (C_1), and two diodes (D_1, D_2). To achieve high voltage boost ability, one diode (D_3) and one capacitor (C_3) are added in the middle part of the circuit. In other words, the input and output ports of the circuit are connected by an impedance source network. This structure brings many attractive advantages such as continuous input current, simple control circuit, high voltage boost ability, wide duty cycle control range, low switching power losses, and maximal usage of the input DC source.

Modes of operation of the proposed converter

MODE I [t_0 to t_1]:

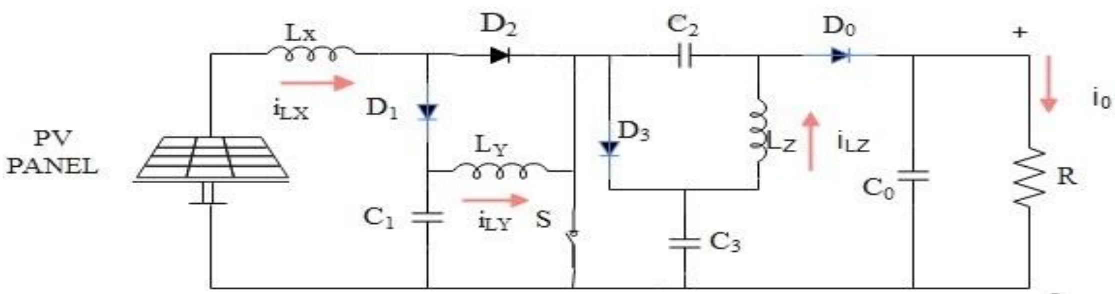

Fig:4: Circuit diagram for MSC converter mode I.

The power circuitry of the proposed converter in mode I is shown in Fig. 1. In mode I, the single switch S operates in conducting mode, and diode D_2 is turned ON by input supply, whereas, diodes D_1, D_3, and D_0 are reverse-biased by capacitors C_1, C_3, and C_0, respectively. Input inductor L_X is charged by input source (V_{in}) with the current path of $V_{in} - L_X - D_2 - S - V_{in}$. The inductor L_Y of the voltage-boosting module is energised by capacitor C_1 with the current path of $C_1 - L_Y - S - C_1$. Similarly, inductor L_Z is magnetised through the current path as $L_Z - C_2 - S - C_3 - L_Z$. However, the load is powered by capacitor C_0, which is isolated from the input source. In this state, currents of inductors increase with a positive current.

MODE II [t_1 to t_2]:

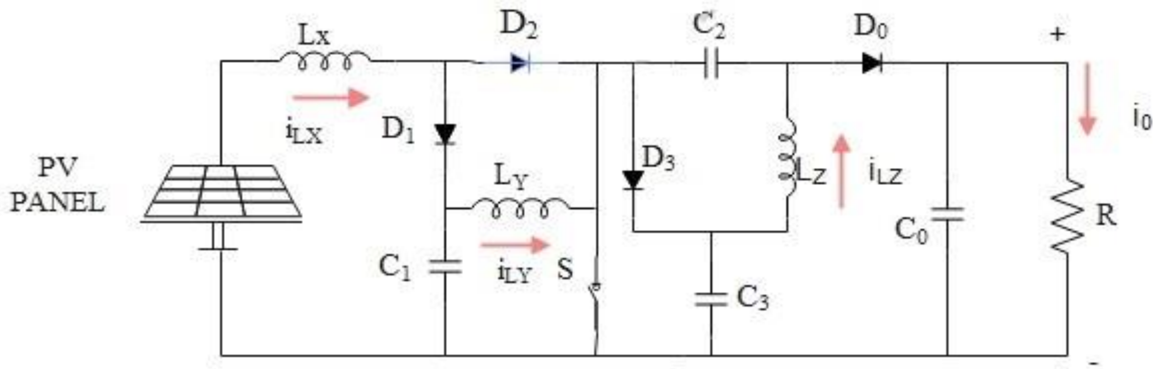

Fig:5: Circuit diagram for MSC converter mode II

The power circuitry of the proposed converter in mode II is shown in Fig. 1. In mode II, switch S is turned OFF and diode D_2 is reverse biased by capacitor C_1. Input inductor L_X transfers its stored energy to capacitor C_1 with the current path $V_{in} - L_X - D_1 - C_1 - V_{in}$. Capacitor C_2 is charged by inductor L_Y through the path $C_1 - L_Y - C_2 - D_0 - C_0 - C_1$. At the same instant, stored energy in inductor L_Z is transferred to capacitor C_3 and load through the path $C_3 - L_Z - D_0 - V_0 - C_3$. In this mode, inductors currents are decreased with a negative. According to Fig. 1 and by applying Kirchhoff's Voltage Law (KVL), circuit expressions can be derived as,

$$L_X \frac{di_{LX}}{\mathrm{dt}}\mathrm{dt} = V_{in} - V_{C1} \quad (1)$$

$$L_Y \frac{di_{LY}}{\mathrm{dt}} = V_{C1} - V_{C3} = V_{C1} + V_{C2} - V_{C0}$$

$$L_Y \frac{di_{LY}}{\mathrm{dt}} + L_Z \frac{di_{LZ}}{\mathrm{dt}} = V_{C1} - V_{C0}$$

$$L_Z \frac{di_{LZ}}{\mathrm{dt}} = V_{C3} - V_{C0} \quad (2)$$

$$C_1 \frac{\mathrm{d}V_{C1}}{\mathrm{dt}} = -i_{LX}$$

$$C_2 \frac{\mathrm{d}V_{C2}}{\mathrm{dt}} = -i_{LY}$$

$$C_3 \frac{\mathrm{d}V_{C3}}{\mathrm{dt}} = -i_{LY}$$

$$C_0 \frac{\mathrm{d}V_{C0}}{\mathrm{dt}} = i_{LZ} - \frac{V_0}{\mathrm{R}} \tag{3}$$

IV. ANALYSIS OF THE PROPOSED CONVERTER

For the analysis of the proposed converter under ideal conditions, it is assumed that the converter system is lossless. The losses of the power diodes, switch, inductors, and source are to be neglected. Moreover, the voltage ripple across each capacitor is small and neglected. According to the inductor voltage second balance law for inductors L_X, L_Y, and L_Z, the ideal voltage expression across the capacitors C_1, C_2, C_3, and C_0 is derived with respect to the input voltage (V_{in}) and duty ratio (k) as,

$$\frac{V_{C1}}{V_{in}} = \frac{1}{(1-k)} \tag{4}$$

$$\frac{V_{C2}}{V_{in}} = \frac{k}{(1-k)^2} \tag{5}$$

$$\frac{V_{C3}}{V_{in}} = \frac{1}{(1-k)^2} \tag{6}$$

$$\frac{V_{C0}}{V_{in}} = \frac{(1+k)}{(1-k)^2} \tag{7}$$

According to equation (7), the ideal voltage gain of the proposed converter in is expressed as

$$V_{LX} = L_X \frac{di_{LX}}{\mathrm{dt}} = V_{in} \qquad V_{LY} = L_Y \frac{di_{LY}}{\mathrm{dt}} = V_{C1}$$

$$V_{LZ} = L_Z \frac{di_{LZ}}{\mathrm{dt}} = V_{C3} - V_{C2}$$

$$C_1 \frac{dV_{C1}}{dt} = i_{LX}, \quad C_2 \frac{dV_{C2}}{dt} = -i_{LZ},$$

$$C_3 \frac{dV_{C3}}{dt} = i_{LZ}, \quad C_0 \frac{dV_{C0}}{dt} = -\frac{V_0}{R}$$

$$\boldsymbol{M} = \frac{\boldsymbol{V_0}}{\boldsymbol{V_{in}}} = \frac{\mathbf{(1+k)}}{\mathbf{(1-k)^2}} \tag{8}$$

Voltage stress on switches and diodes

According to the aforementioned analysis and it is observed that the voltage stress across switch S is equal to the voltage across capacitor C_3 in mode II and carrying current equal to the addition of all three inductor currents in mode I, which can be expressed in terms of output voltage and duty ratio as

$$V_{D1} = \frac{V_0}{(1 + k)}$$

$$I_S = I_{LX} + I_{LY} + \mathrm{I_{LZ}} \tag{9}$$

However, the peak inverse voltage (PIV) of diodes D_1 is V_{D1}, which is equal to the voltage across capacitor C_1. Similarly, the voltage across D_2 (V_{D2}), D_3 (V_{D3}), and D_0 (V_{D0}) is equal to the voltage across capacitor C_2, C_3, and C_0, respectively. The PIV across each diode and its respective current carrying capacity can be expressed as

$$V_{D1} = \frac{V_0(1 - k)}{(1 + k)}, \qquad i_{D1} = (i_{Lx})_{(min)} = \frac{V_{in}}{L_X}$$

$$V_{D2} = \frac{V_0 k}{(1 + k)}, \qquad i_{D2} = (i_{LY})_{(min)} = \frac{V_{in} - V_{C1}}{L_X}$$

$$V_{D3} = \frac{V_0}{(1 + k)}, \qquad i_{D2} = (i_{LY})_{(min)} = \frac{V_{C1} + V_{C2} - V_0}{L_Y}$$

$$V_{D0} = \frac{V_0}{(1 + k)}, \qquad i_{D0} = i_0 - i_{C0} \tag{10}$$

Selection of inductors:

The value of inductors is dependent on the applied input voltage, duty ratio, inductor ripple current, and switching frequency. By applying the ampere second balance principle on the capacitor and (3), the average current (I_{LX}, I_{LY}, and I_{LZ}) and the ripple current (Δi_{LX}, Δi_{LY}, and Δi_{LZ}) of inductors are expressed as

$$\Delta i_{LX} = \frac{kV_{in}}{L_X f_s} \qquad I_{LX} = \frac{(1+k)^2 V_{in}}{(1-k)^4 R}$$

$$\Delta i_{LY} = \frac{kV_{in}}{(f_s(1 - k)L_Y)} \qquad I_{LY} = \frac{(1 + k)^2 V_{in}}{(1 - k)^3 R}$$

$$\Delta i_{LZ} = \frac{K^2 V_{in}}{(f_s(1-k)^2 L_Z)} \qquad I_{LZ} = \frac{(1+k)^2 V_{in}}{(1-k)^2 R} \tag{11}$$

where i_{LX}, i_{LY}, and i_{LZ} are currents through inductors L_X, L_Y, and L_Z respectively. f_s is the switching frequency and R is the resistive load.

To operate the proposed converter in CCM, the value of inductors should be selected more than the respective critical inductance value. The critical inductance is calculated as follows:

$$(L_X)c > \frac{k(1 - k)^4 R}{2(1 - k)^2 f_s}$$

$$(L_Y)c > \frac{k(1 - k)^2 R}{2(1 + k)^2 f_s}$$

$$(L_Z)c > \frac{K^2 R}{2(1 + k)^2 f_s} \tag{12}$$

Selection of capacitors

The capacitor (C_0–C_3) design is dependent on the applied input voltage, duty cycle, and voltage ripples (Δ_{VC}). For good design, it is considered that the voltage ripple in the capacitor voltage is 1% of the total input voltage. The critical capacitance of capacitors C_0– C_3 is calculated as follows:

INTERNATIONAL SCIENTIFIC JOURNAL OF ENGINEERING AND MANAGEMENT ISSN: 2583-6129
VOLUME: 03 ISSUE: 06 | JUNE – 2024 DOI: 10.55041/ISJEM02089
AN INTERNATIONAL SCHOLARLY || MULTIDISCIPLINARY || OPEN ACCESS || INDEXING IN ALL MAJOR DATABASE & METADATA

$$(C_1)_C = \frac{V_{C1}k}{R\Delta V_{C1}f_s} = \frac{V_{in}\ k}{(1 - k)RC1\ f_s}$$

$$(C_2)_C = \frac{V_{C2}k}{R\Delta V_{C2}f_s} = \frac{V_{in}K^2}{(1-k)^2 R\Delta V_{C2}\ f_s}$$

$$(C_3)_C = \frac{V_{C3}k}{R\Delta V_{C3}f_s} = \frac{V_{in}\ k}{(1 - k)^2 R\Delta V_{C3}\ f_s}$$

$$(C_0)c = \frac{V_{C0}k}{R\Delta V_{C0}f_s} = \frac{V_0\ k}{R\Delta V_{C0}\ f_s} \tag{13}$$

The voltage rating of capacitors C_1, C_2, C_3, and C_0 is decided and calculated from (4) to (7), respectively.

TABLE NO:1 DESIGN PARAMETERS OF THE PROPOSED CONVERTER:

SI.NO	**Parameters**	**Prototype**
1.	Power	600 W
2.	Input voltage (V_{in})	30 V
3.	Duty ratio	D = 0.7
4	Switching freq.	50 kHz
5.	Inductors L_X, L_Y, and L_Z	100 µH,
6.	Capacitor C_1,C_3	100 µF
7.	Capacitor C_2,C_0	100 µF
8.	Output voltage (V_0)	500V

INTERNATIONAL SCIENTIFIC JOURNAL OF ENGINEERING AND MANAGEMENT ISSN: 2583-6129
VOLUME: 03 ISSUE: 06 | JUNE – 2024 DOI: 10.55041/ISJEM02089
AN INTERNATIONAL SCHOLARLY || MULTIDISCIPLINARY || OPEN ACCESS || INDEXING IN ALL MAJOR DATABASE & METADATA

SIMULATION CIRCUIT DIAGRAM FOR MSC CONVERTER

The modeling of of PV based modified sepic converter for microgrid applications is designed in MATLAB/SIMULINK and output result is obtained.

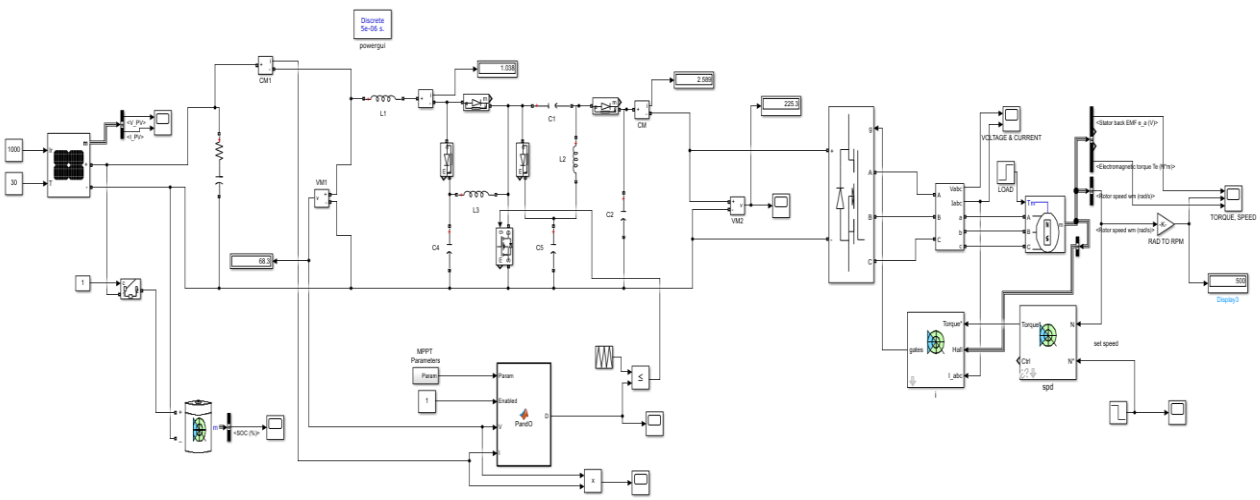

Fig:6: Simulation circuit diagram for MSC Converter.

V. SIMULATION RESULTS:

Simulation result of PV system

Simulation waveform for input voltage and current.

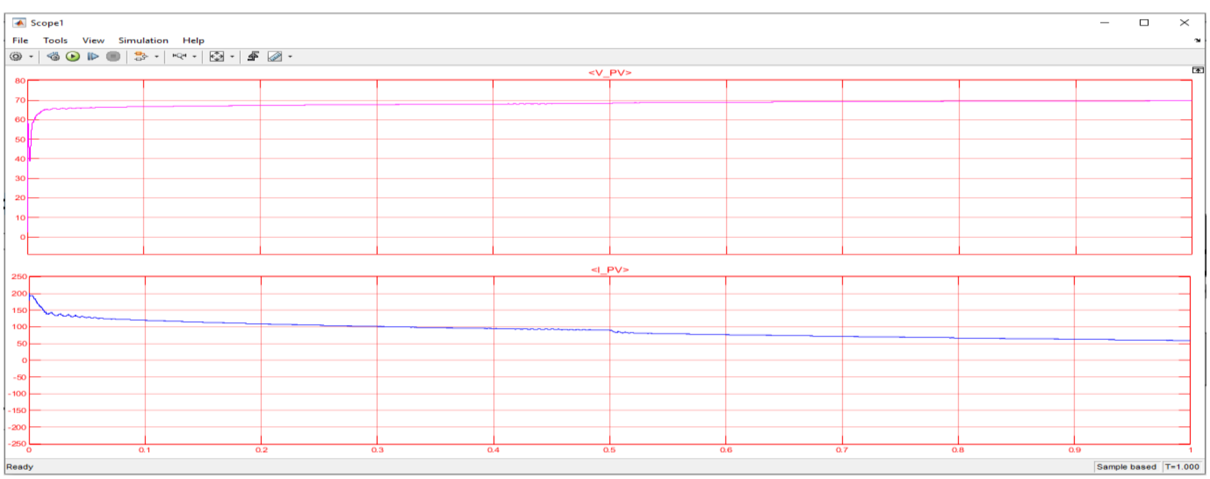

Fig:7: Waveform for input voltage and current.

It is observed two line in fig 7 that the PV voltage remains constant and it is fed to the MSC.

INTERNATIONAL SCIENTIFIC JOURNAL OF ENGINEERING AND MANAGEMENT ISSN: 2583-6129
VOLUME: 03 ISSUE: 06 | JUNE – 2024 DOI: 10.55041/ISJEM02089
AN INTERNATIONAL SCHOLARLY || MULTIDISCIPLINARY || OPEN ACCESS || INDEXING IN ALL MAJOR DATABASE & METADATA

Simulation result of MSC:

Simulation waveform for MSC converter output.

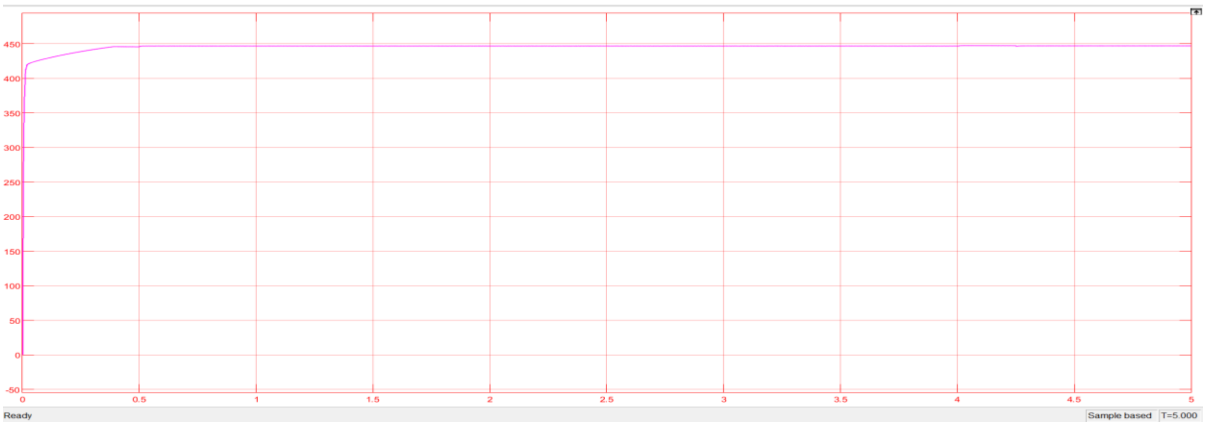

Fig:8: output waveform for MSC converter voltage.

Fig 8 shows the output waveform of the MSC. It is further fed to the BLDC motor.

Simulation result of BLDC V&I Measurement:

Simulation waveform for three phase voltage measurement and current.

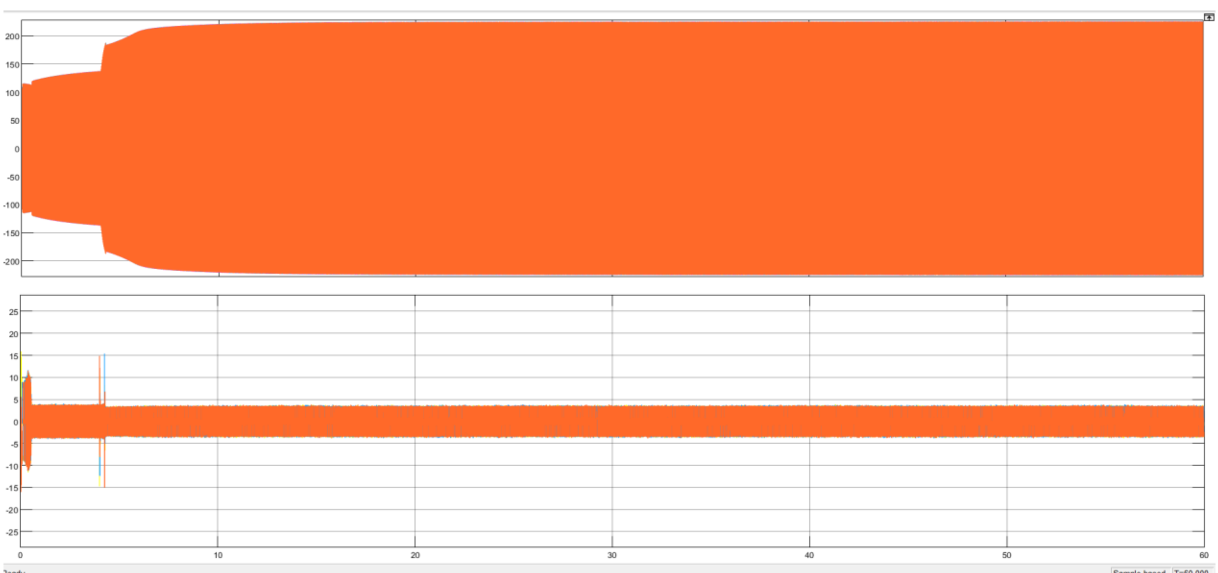

Fig:9: Output waveform for voltage and current.

It is observed two line in fig 9 that the BLDC Motor voltage and current remains constant and it is fed to the MSC

Simulation result of BLDC Torque, Speed, EMF:

Simulation waveform for torque and speed and EMF.

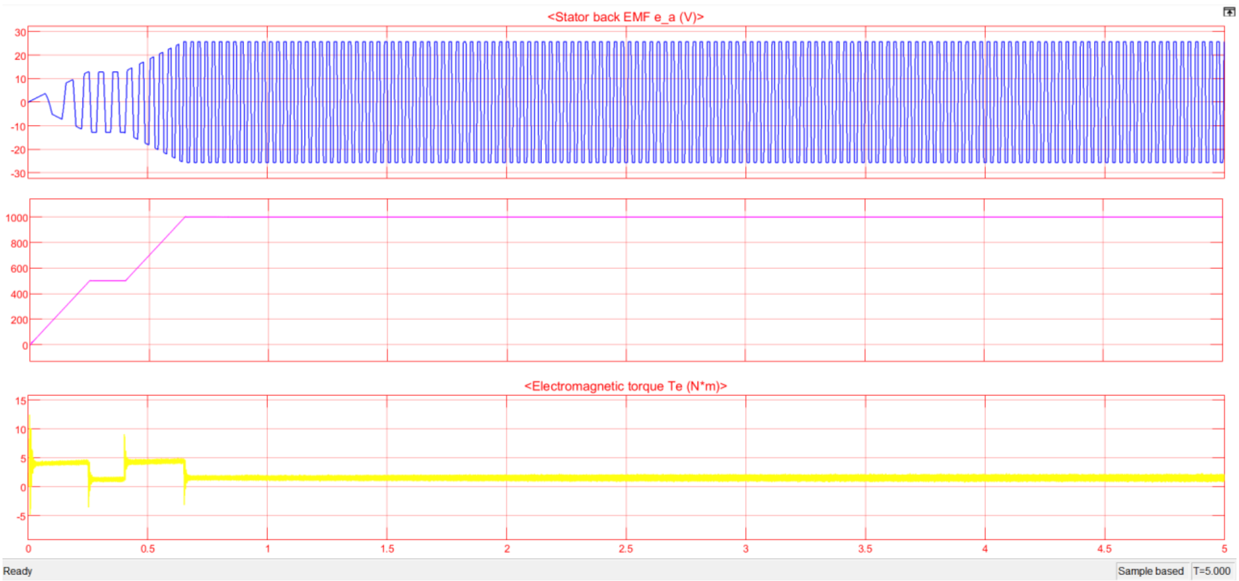

Fig:10: Output waveform for BLDC motor torque and speed and EMF.

It is observed three line in fig 10 that the BLDC Motor Torque and Speed and EMF.

VI. CONCLUSIONS

In this paper PV Based Modified SEPIC Converter Fed BLDC motor for Electric Vehicle was developed. The proposed converter utilises a single switch in its structure, which results in simple control and switching power losses reduction. The voltage-boosting module and a modified SEPIC structure were utilised in the presented topology to attain high-output voltage required for a EV application with a practical duty cycle. Furthermore, the presented topology drains a continuous current from the input supply. Hence, high-voltage boost ability and continuous input current make it suitable for PV applications. Moreover, the voltage stress across the switch and load side diode is less than the output voltage and comparatively low as compared to other converters. In general, the proposed converter can be presented as a good complement of high-voltage gain DC–DC converters. The performance of PI, MPPT controller are also analysed. The simulation result of PV system, MSC, BLDC Motor parameters are convincing and ready for hardware implementation.

VII. ACKNOWLEDGEMENTS

The authors acknowledge the facilities rendered by the Government Collage of Engineering, Salem For carrying out this work.

VIII. REFERENCES

[1] U. Shahzad, "The need for renewable energy sources," International Journal of Information Technology and Electrical Engineering, vol. 2, 2017.

[2] E. Mclamb, "Fossil fuels vs. renewable energy resources," 2011, [Accessed 20th April 2015], http://www.ecology.com/2011/09/ 06/fossil-fuels renewable-energy-resources/.

[3] C. J. Anders, "Greatest fossil fuels disasters in human history," 2010, [Accessed 20th April 2015], http://io9.com/5526826/ greatest-fossil-fuel-disasters-inhuman-history.

[4] D. Kumar, F. Zare, and A. Ghosh, "DC Microgrid technology: system architectures, AC grid interfaces, grounding schemes, power quality, communication networks, applications, and standardizations aspects," IEEE Access, vol. 5, article 12230, 2017.

[5] T. Dragičević, X. Lu, J. C. Vasquez, and J. M. Guerrero, "DC microgrids—part i: a review of control strategies and stabilization techniques," IEEE Transactions on Power Electronics, vol. 31, no. 7, pp. 4876–4891, 2016.

[6] N. Yang, B. Nahid-Mobarakeh, F. Gao, D. Paire, A. Miraoui, and W. Liu, "Modeling and stability analysis of multi-time scale DC microgrid," Electric Power Systems Research, vol. 140, pp. 906–916, 2016.

[7] M. Nymand and M. A. E. Andersen, "High-efficiency isolated boost DC–DC converter for high-power low-voltage fuel-cell applications," IEEE Transactions on Industrial Electronics, vol. 57, no. 2, pp. 505–514, 2010.

[8] Tomaszuk, T., Krupa, A.: 'High-efficiency high step-up DC/DC converters – a review', Bull. Polish Acad. Sci., 2011, 59, (4), pp. 475–483.

[9] Cornea, O., Andreescu, G., Muntean, N., et al.: 'Bidirectional power flow control in a DC microgrid through a switched-capacitor cell hybrid DC–DC converter', IEEE Trans. Ind. Electron., 2017, 64, (4), pp. 3012–3022.

[10] Li, W., He, X.: 'Review of non-isolated high-step-up DC/DC converters in photovoltaic grid-connected applications', IEEE Trans. Ind. Electron., 2011, 58, (4), pp. 1239–1250.

[11] Blaabjerg, F., Kjaer, S.B.: 'Power electronics as efficient interface in dispersed power generation systems', IEEE Trans. Power Electron., 2004, 19, (5), pp. 1184–1194.

[12] Tofoli, F.L., de Castro Pereira, D., de Paula, W.J., et al.: 'Survey on nonisolated high-voltage step-up DC–DC topologies based on the boost converter', IET Power Electron., 2015, 8, (10), pp. 2044–2057.

[13] Gules, R., dos Santos, W.M., dos Reis, F.A., et al.: 'A modified SEPIC converter with high static gain for renewable applications', IEEE Trans. Power Electron., 2014, 29, (11), pp. 5860–5871.

[14] Tang, Y., Fu, D., Wang, T.: 'Hybrid switched-inductor converters for high step-up conversion', IEEE Trans. Ind. Electron., 2015, **62**, (3), pp. 1480–1490.

[15] Adib, A.; Shadmand, M.B.; Shamsi, P.; Afridi, K.K.; Amirabadi, M.; Fateh, F.; Ferdowsi, M.; Lehman, B.; Lewis, L.H.; Mirafzal, B.; et al. E-Mobility-Advancements and Challenges. IEEE Access **2019**, 7, 165226–165240.

[16] Mohammed, S.S.; Ahamed, T.I.; Aleem, S.H.A.; Omar, A.I. Interruptible Charge Scheduling for Plug-In Electric Vehicle to Minimize Charging Cost Using Heuristic Algorithm. Electr. Eng. **2021**, 104, 1425–1440.

[17] Titus, F.; Thanikanti, S.B.; Deb, S.; Kumar, N.M. Charge Scheduling Optimization of Plug-In Electric Vehicle in a PV Powered Grid-Connected Charging Station Based on Day-Ahead Solar Energy Forecasting in Australia. Sustainability **2022**, 14, 3498.

[18] Affam, A.; Buswig, Y.M.; Othman, A.-K.B.H.; Bin Julai, N.; Qays, O. A review of multiple input DC-DC converter topologies linked with hybrid electric vehicles and renewable energy systems. Renew. Sustain. Energy Rev. **2020**, 135, 110186.

[19] Aravindha Shilpa K, Swaroopa K, PV based Sepic Converter FED Electric Vehicle Design using MABLAB/Simulink **2021** P 2395-0072

[20] Jyothi B, Bhavana P, Thirumala Rao B, Mukesh Pushkarna, Kitmo ,and Repele Djidimbele, Implementation of Modified SEPIC Converter for Renewable Energy Built DC Microgrids **2023** 2620367.